PREDICTIVE CONTROL STRATEGIES FOR VARIABLE SPEED WIND TURBINE WITH SATURATED INDUCTION GENERATOR

Soufiane MEDDOURI [1,2]. Le Anh DAO[1]
[1] Dip.to di Elettronica, Informazione e Bioingegneria, Politecnico di Milano
Piazza L. da Vinci 32, 20133 Milano (Italy), soufiane.meddouri@polimi.it, leanh.dao@polimi.it
[2] Laboratoire de Technologie Industrielle et de l'Information Faculté, de Technologie,
Université de Bejaia, 06000 Bejaia, (Algeria)

Luca FERRARINI[1]
[1] Dip.to di Elettronica, Informazione e Bioingegneria, Politecnico di Milano
Piazza L. da Vinci 32, 20133 Milano (Italy), Phone +39 02 2399 3672, luca.ferrarini@polimi.it

Abstract: *This paper proposes a Model Predictive Control (MPC) scheme combined with rotor flux-oriented control principal for a self-exited induction generator driven by a variable speed wind turbine in a stand-alone system. The excitation of the autonomous squirrel cage induction generator is achieved by means of PWM inverter/rectifier with a single capacitor, where the saturation effect of the magnetic circuit of the induction generator is taken into account and modeled as a variable inductance as function of the magnetic current. Effective approaches are proposed, namely the switched and adaptive MPC, to take into account large variations of important parameters. The objective is to keep the DC voltage at the rectifier output and the rotor flux constant and equal to the reference value regardless of different disturbances, like wind speed, load and parameter uncertainties of the induction generator. A wide analysis and comparison of simulation results are provided to check the effectiveness of the proposed MPC controller under different operating conditions, also considering a variety of control options.*

Key words: *Adaptive MPC, Induction Generator, Saturation effect, Renewable energy.*

1. Introduction.

The interest in the use of renewable energy in recent years has increased significantly, because people are increasingly concerned with environmental issues. These energies include wind power which represents a huge resource with more than 54 GW of power installed across the global market in 2016, its capacity has expanded rapidly to 486.8 GW, cumulative capacity grew by 12.6% [1]. Clearly such an increase is mainly due the presence of large mass production plants connected to the grid which is the most dominant and visible aspect. However, along with the high-power wind generation, small power systems are under development especially for isolated sites or in an urban environment, also with the appearance of the new architectures.

For stand-alone wind turbines, different electrical machines can be used to fulfill the electromechanical conversion task. Induction Generators (IGs) are responding and extensively used in industrial applications, mainly due to their known advantages like robustness, small size, low maintenance cost and especially its capability to start without an external reactive power source, which is useful in stand-alone power generating systems where the reactive power from the grid is not available [2-6]. The simplest and cheapest way to use it as an autonomous generator consists in connecting its stator windings to a capacitor bank in parallel to the load. The remaining magnetic flux, added to the magnetizing current through the capacitor bank yields the construction of the electromotive force and it increases to a useful value. This approach is useful and sufficient to convert the wind energy into electrical one for isolated or faraway areas from the distribution grid [3]. However, the main negative effect of this kind of generator consists in its inherently poor voltage regulation for both speed and load variation. Thus, it is mandatory to have an appropriate and robust voltage control scheme. Different voltage control schemes have been proposed for this purpose in the technical literature, where usually the generator models used have been obtained under different simplification assumptions which do not represent the real case of the induction generator model [4-6].

Since many years, the field-oriented control is largely used for controlled electrical drives, it has been proved as the algorithm that gives the best performances and dominantly applied in Self-Excited Induction Generator (SEIG) systems, simply because of the advantages of this strategy which has superior dynamic control features. Most of such systems use classical PI controllers [4-10], due to the simplicity

of the structure and ease of the design. However, the performance obtained by a PI controller is sensitive to plant parameter variations and external disturbances [11]. In [4-6], the DC voltage control is achieved by connecting a rectifier/inverter system to the stator windings of the isolated IG.

Artificial intelligence techniques such as Fuzzy Logic also have been applied to the control of wind energy conversion systems [12-14]. Fuzzy DC voltage control has been proposed in [12], and a comparison with classical PI was provided. One of the advantages with respect to other conventional controllers like the classical PI controllers is the capability of handling uncertain and noisy signals and the fact that they do not require the knowledge of a detailed mathematical model of the system under control [13]. In [14], fuzzy vector control strategy has been proposed to regulate the DC voltage of IG taking the saturation effect into account, but with limited range of speed variation. However, these methods do not offer good transient performance with respect to the advanced control technique like Model Predictive Control.

Sliding mode control is also used to control wind energy conversion system based induction generator [15, 16]. In [16] direct torque and rotor flux control (DTRFC) algorithm based on the sliding mode approach was proposed in case of small changes of wind and load variation. However, this approach does not offer good performances especially in case of load variation.

Model Predictive Control (MPC) has been developed considerably over the last few years since it proved to be an efficient control strategy in many applications. It can provide a good performance in largely different systems and processes under uncertainties, nonlinear and multi-variable systems, in particular in energy conversion [17]. Typically, MPC controller requires a significant computational effort. Nevertheless, nowadays MPC can be applied to rapid systems with shorter sampling time as electrical drives [18], thanks to the development of fast hardware. Hence, many researchers have been using the MPC strategy for electrical drives [17-22], where the nonlinearity of the magnetic circuit is always neglected. In [19], an application of MPC to control the voltage and frequency was proposed for a standalone generation system achieved by connecting a static VAR at the generator terminal for voltage regulation, where the generator terminal voltage depends mainly on the static VAR capacitance, rotor speed and the load impedance. In [20], an MPC of permanent magnet synchronous motor has been introduced with unknown load torque using a linear plant model. Another MPC strategy called predictive torque control has been introduced in [21-22]. In [23], a comparison between field-oriented control and predictive torque control is presented and applied to induction machines in both simulation and experimental tests. All the above mentioned results show the effectiveness of the MPC application to the electrical drives control problems.

This paper investigates the successful application of an innovative MPC control scheme using MPC single model strategy (i.e., based on a single model), switched MPC strategy and adaptive MPC strategy, which are based on rotor field oriented control principle applied to a self-induction generator with a squirrel cage induction generator driven by a variable wind speed, feeding different load values. An additional level of complexity in the system addressed in the present paper is the saturation effect of the magnetic circuit taken into account, which is modeled as a variable magnetizing inductance as a function of the magnetizing current [14]. A further complexity is that we want to insure the tracking of both DC voltage and rotor flux regardless of the variable rotor speed, load variation and parameter uncertainties of the generator model, considering large variations of the parameters. Preliminary results, with no adaptation and limited range of driving speed of the IG, have been illustrated in [25], while performance analysis of the considered system under different disturbances have been preliminarily investigated in [26] with no adaptation as well. Before starting the comparison between different control strategies using MPC technique here proposed, we give a brief comparison between MPC based single model and fuzzy logic control strategy in terms of DC voltage control in case of rotor speed changes.

The paper is structured as follows. Section 2 describes the system under investigation and its mathematical formulation. Section 3 is devoted to show the application of the basic concepts of MPC to control the IG behavior, while section 4 extends the control technique to switched and adaptive control. The results obtained are discussed in Section 5, to analyze in detail the impact of the load changes (sect. 5.1), the impact of the rotation speed changes (sect. 5.2). A case study IG is considered whose parameters are presented in the Appendix.

2. System description and modeling.

2.1. System description.

The SEIG system studied in this work with the control scheme is depicted in Fig. 1. It is composed mainly of squirrel cage induction generator (SCIG) driven by variable wind turbine speed, a PWM converter connected to a single capacitor to excite the IG with a battery in order to start up the system, an isolated load represented here as resistance R, and a diode to decouple the rectifier from the battery as soon as the voltage generated at the output of the rectifier is higher than the battery side.

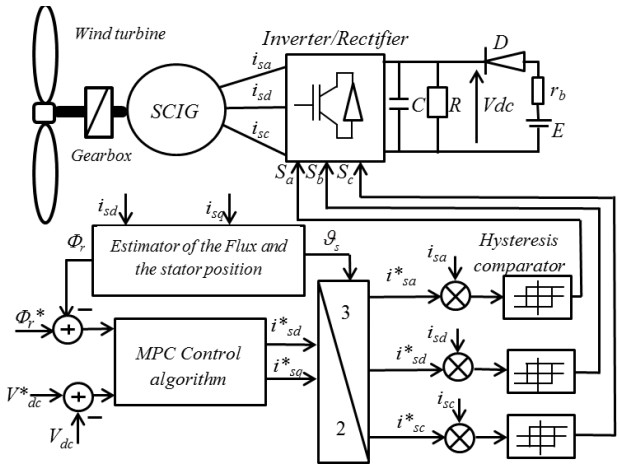

Fig.1. The studied system.

2.2. Induction generator modeling

In order to study the system performances with a good accuracy, the induction generator model used in this work takes the saturation effect of the magnetic circuit into account. It is modeled as a variable inductance as function of the magnetic current, and approximated with a polynomial function of degree 12. The electrical equations are given in equation (1) according to the d-q model as following: (for more details, see [14, 24]):

$$\begin{bmatrix} v_{sd} \\ v_{sq} \\ 0 \\ 0 \end{bmatrix} = \begin{bmatrix} R_s & -P\Omega\, l_s & 0 & -P\Omega\, L_m \\ P\Omega\, l_s & R_s & P\Omega\, L_m & 0 \\ -R_r & 0 & R_r & 0 \\ 0 & -R_r & 0 & R_r \end{bmatrix} \cdot \begin{bmatrix} i_{sd} \\ i_{sq} \\ i_{md} \\ i_{mq} \end{bmatrix}$$

$$+ \begin{bmatrix} l_s & 0 & L_m + L_m' \cdot \frac{i_{md}^2}{|i_m|} & L_m' \cdot \frac{i_{md} \cdot i_{mq}}{|i_m|} \\ 0 & l_s & L_m' \cdot \frac{i_{md} \cdot i_{mq}}{|i_m|} & L_m + L_m' \cdot \frac{i_{mq}^2}{|i_m|} \\ -l_r & 0 & l_r + L_m + L_m' \cdot \frac{i_{md}^2}{|i_m|} & L_m' \cdot \frac{i_{md} \cdot i_{mq}}{|i_m|} \\ 0 & -l_r & L_m' \cdot \frac{i_{md} \cdot i_{mq}}{|i_m|} & l_r + L_m + L_m' \cdot \frac{i_{mq}^2}{|i_m|} \end{bmatrix} \cdot \begin{bmatrix} \frac{di_{sd}}{dt} \\ \frac{di_{sq}}{dt} \\ \frac{di_{md}}{dt} \\ \frac{di_{mq}}{dt} \end{bmatrix} \quad (1)$$

where P is the pole pair number, Ω is the mechanical speed of the machine. R_s, l_s and R_r, l_r are the stator and rotor phase resistances and leakage inductances respectively, L_m is the magnetizing inductance. V_{sd}, i_{sd}, V_{sq} and i_{sq} are the *d-q* stator voltages and currents respectively. i_{md} and i_{mq} are the magnetizing currents, along the *d* and *q* axis, given by the following equation:

$$\begin{cases} i_{md} = i_{sd} + i_{rd} \\ i_{mq} = i_{sq} + i_{rq} \end{cases} \quad (2)$$

The curve of magnetizing inductance (L_m) as a function of the current i_m is given in Fig. 2.

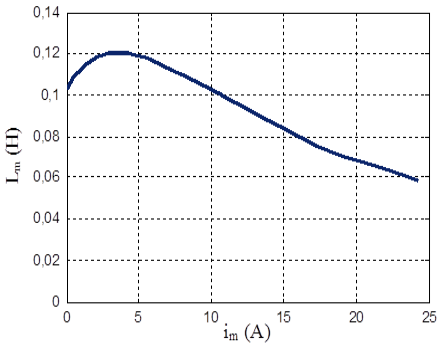

Fig.2. Magnetizing inductance curve.

3. Predictive Control strategy

3.1. Decoupling with Vector Control

The total absence of decoupling between the flux and the torque in the asynchronous machine poses difficult problems for its control. For this reason, a vector control principle in particular the rotor flux oriented control is exploited in this paper ($\Phi_{rd} = \Phi_r$ and Φ_{rq}=0), where the main target is to assimilate the induction motor to a DC motor by controlling the flux and the torque separately.

The electromagnetic torque is given by equation (3) where *P* and *M* are the pair pole number and mutual inductance respectively:

$$T_{em} = P \frac{M}{L_r} i_{sq} \Phi_r \quad (3)$$

The estimated rotor flux is expressed in equation(4) as a function of stator current i_{sd} and rotor time constant *Tr*, where *Tr=Lr/Rr*

$$\Phi_r = \frac{M i_{sd}}{1 + T_r s} \quad (4)$$

where *s* is differential (*Laplace*) operator. The estimation of the stator pulsation is given by the following equation where Ω represents the mechanical speed:

$$w_s = \frac{M i_{sq}}{T_r \Phi_r} + P\Omega \quad (5)$$

3.2. Model Predictive Control

In order to control the DC voltage at rectifier output (V_{dc}) and flux (Φ_r), Model Predictive Control (MPC) strategy is proposed. Basically, as shown in Fig. 3, an MPC architecture is composed of two main components: the system model and an optimizer.

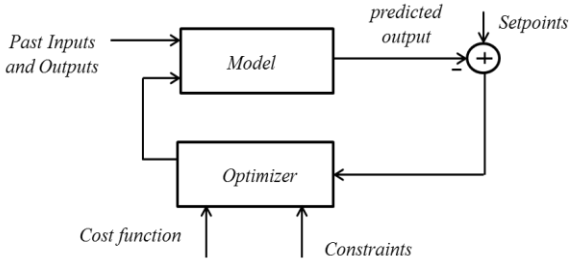

Fig.3. Typical MPC scheme.

The purpose of having a model is to mathematically represent the relationship between outputs and inputs of the plant to perform optimization. However, achieving an exact model of a plant is practically impossible, especially with the highly nonlinear plant at hand due to the saturation effect, hysteresis control, etc. Hence, an estimated system model based on step response identification around an equilibrium point is numerically constructed. In our consideration, the changes of V_{dc} (*i.e.*, ΔV_{dc}) with respect to the step changes of inputs (*i.e.*, Δw, Δi_{sd} and Δi_{sq}) around an equilibrium point is derived which basically illustrates how V_{dc} changes if there are variations of inputs, as hinted in fig. 4. Similarly, for the change of Φ_r (*i.e.*, $\Delta\Phi_r$) with respect to the same step variations of the inputs. Applying the method to the considered case study IG, the transfer functions of the system are derived as follows:

$$G_{\Delta isd-\Delta\Phi} = 0.1047\frac{1}{1+0.0847s}$$

$$G_{\Delta isd-\Delta Vdc} = \frac{84.708\,(1+0.002s)}{(1+0.069s)(1+0.087s)}$$

$$G_{\Delta isq-\Delta Vdc} = -18.3588\frac{1}{1+0.0695s} \quad (6)$$

$$G_{\Delta w-\Delta Vdc} = 1.8867\frac{1}{1+0.0695s}$$

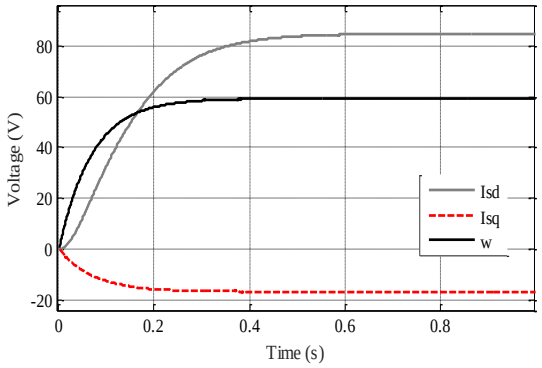

Fig.4. Superposition principle checking

Then, the typical discrete state space model is accordingly built as follows:

$$\begin{cases} x_{k+1} = Ax_k + Bu_k + B_d d_k \\ y_k = Cx_k + Du_k \end{cases} \quad (7)$$

The future behavior of the plant is afterward predicted as functions of the inputs following the Dynamic Matrix Control (DMC) framework in the following expression.

$$\hat{Y} = \begin{bmatrix} CA \\ CA^2 \\ \vdots \\ CA^{Hp} \end{bmatrix} \hat{x}_{k|k} +$$

$$\begin{bmatrix} CB \\ CAB + CB \\ \vdots \\ \sum_{i=1}^{Hp} CA^{i-1}B \end{bmatrix} u_{k-1} + \begin{bmatrix} CB \\ CAB + CB \\ \vdots \\ \sum_{i=1}^{Hp} CA^{i-1}B \end{bmatrix} \Delta w_k + \begin{bmatrix} I \\ I \\ \vdots \\ I \end{bmatrix} \hat{p}_{k|k} \quad (8)$$

$$+ \begin{bmatrix} CB & 0 & \cdots & 0 \\ CAB + CB & CB & 0 & 0 \\ \vdots & \vdots & \vdots & \vdots \\ \sum_{i=1}^{Hp} CA^{i-1}B & \sum_{i=1}^{Hp-1} CA^{i-1}B & \cdots & \cdots \end{bmatrix} \Delta u$$

where $\hat{Y}$ is vector of future outputs prediction over prediction horizon (H_p), $\hat{x}_{k|k}$ is estimated values of state variables, u_{k-1} presents the latest actual control actions; Δu is vector of future control actions increments, $\hat{p}_{k|k}$ is considered as output correction term as it equals to the difference between the current output and the predicted current output at previous time instant.

As for the mechanical pulsation, a prediction for Δw is not performed as it is considered to be equal to current value Δw_k. A, B, C, D and B_d are system matrices in discrete state space model as presented in equation (7). Notice that all values are taken into account at current time *k*. Now, the control problem can be transformed into an optimization problem taking into account different and sometimes conflicting goals subject to system constraints. The cost function is presented as a weighted sum of four different quadratic terms $J^{R,isq}$, $J^{R,isq}$, J^V, J^F. They respectively account for smoothing Δi_{sd}, smoothing Δi_{sq}, tracking ΔV_{dc} and tracking $\Delta\Phi$. Their corresponding weights are named as $w^{R,isd}$, $w^{R,isq}$, w^V and w^F. Notice that all the weights are designed with respect to normalized values of inputs and outputs. In more detail, the cost function terms here considered are the quadratic forms described in the following format:

$$J = w^{R,isd}J^{R,isd} + w^{R,isq}J^{R,isq} + w^V J^V + w^F J^F \quad (9)$$

$$J^{R,isd} = \sum_{i=0}^{H_c-1} (\Delta i_{sd,k+i|k} - \Delta i_{sd,k+i-1|k})^2$$

$$J^{R,isq} = \sum_{i=0}^{H_c-1} (\Delta i_{sq,k+i|k} - \Delta i_{sq,k+i-1|k})^2$$

$$J^{V} = \sum_{i=1}^{H_p} (\Delta V^*_{dc,k+i} - \Delta \hat{V}_{k+i|k})^2$$

$$J^{F} = \sum_{i=1}^{H_p} (\Delta \Phi^*_{k+i} - \Delta \hat{\Phi}_{k+i|k})^2$$

where $\Delta V^*_{dc,k+i}$ and $\Delta \Phi^*_{k+I}$ are the setpoints of ΔV_{dc} and $\Delta \Phi$, respectively, which basically equal to the differences between the setpoints of outputs and its equilibrium values.

Since the outputs can be represented as a linear function of control variables as in equation (8), all the cost terms can be expressed in a form that includes only control variables and constant terms. As for the constraints, the maximum (minimum) values of control variables and the changes of two consecutive control moves are imposed as presented below in Table 3. Since they are directly related to control variables, it is straightforward to express the constraints as a standard linear inequality form. As a conclusion, the optimization problem is can be formulated in a general form as follows:

$$\min_{\Delta u} \Delta u^T A_{o,k} \Delta u + B_{o,k} \Delta u + C_{o,k}$$
$$\text{subject to } D_k \Delta u \leq b_k \tag{10}$$

where D_k and b_k are suitable matrices simply derived from actual constraints at time k and $A_{o,k}$, $B_{o,k}$, $C_{o,k}$ are suitable coefficient matrices related to each term of the cost function at time k.

By solving the optimization problem, the optimizer then provides a series of control actions from current instant till the end of control horizon. Following the receding horizon technique, only the first control sample is applied to the real plant. After that, the optimization problem is reformulated and solved at the next time instant with new updated information from the plant. The superiority of the MPC over traditional control structures is shown in Fig. 5, where a comparison is provided between a straightforward MPC (developed in [25]) and a Fuzzy PID controller (developed in [14]), with an improvement of about 22% (10 v of reduction in the undershoot/overshoot) when the rotation speed changes by 20% below and above the synchronous speed, where we have an improvement in time response also as it can be seen in Fig.5. To improve transient performance, in [26] a special smoothing technique for the reference signals was introduced (for general discussion of the technique see [27]). Briefly, the system is driven to track a trajectory which is constructed as a gradual transition to the desired setpoint as shown below:

$$y_r(k+i|k) = (\alpha_k)^i y(k) + \left[1 - (\alpha_k)^i\right] y_{sp} \quad \forall i = 1,2,\dots,H_p \tag{11}$$

where $y_r(k+i|k)$ is the new reference trajectory after i steps from current time instant k, $y(k)$ is the measured value of y at time k, y_{sp} is the actual setpoint that should be reached by the plant, and H_p is prediction horizon. After some investigations, the parameter α_k has been adaptively changed with time, as a special function of the tracking error:

$$\alpha_k = \frac{1}{1 + 0.097|y(k) - y_{sp}|} \tag{12}$$

where |.| refers to absolute value function.

The basic MPC formulation given in [25, 26] is there applied only with small variations of the rotation speed. The present paper focuses on larger variation of parameters like rotation speed and load, which excites more strongly nonlinear behaviors. In particular, the present paper proposes and analyses new forms of MPC, namely switched and adaptive versions, to better follow the plant dynamics and improve transient results. On top of that, a sensitivity analysis is carried out to find good values of prediction and control steps as a compromise between computational burden and performance. Selected values for prediction and control horizons are 40 and 10 steps respectively.

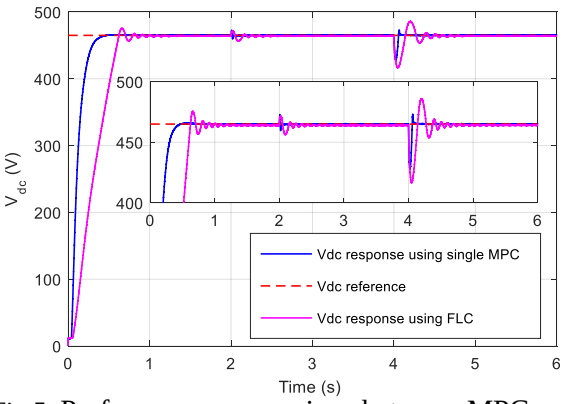

Fig.5. Performance comparison between MPC and PI in DC voltage.

4. Switched and Adaptive Predictive Control

The predictive control strategy relies on a system model developed by using an identification method around an equilibrium point. As mentioned in previous section, the real plant is essentially nonlinear. A single linear system model is rarely a good enough representation of the real plant. In order

to improve the MPC performance which strongly depends on the reliability of the system model, innovative control schemes (a switched and an adaptive MPC) are proposed here, which employ a set of models estimated around different operational points of the system. In these studies, the models are changed simultaneously as soon as any changes of load and rotation speed are recorded.

To construct the set of models, the same identification technique with different values of wind and load is used, as they are main sources of variation in the considered system. In this paper, for the sake of simplicity, four different operational points (P_x, x=1, 2, 3, 4) are considered with respect to four different combinations of wind and load different values as shown in Table 1.

Table 1
Operation points in case of speed and load changes

	P_1	P_2	P_3	P_4
Ω (RPM)	750	900	600	750
R (Ω)	70	70	70	140

Clearly, there will be a set of values of system inputs corresponding to the system outputs specified by P_x in Table 1. The model identified for any P_x is constituted by four transfer functions from system inputs and outputs as described in Table 2. The transfer functions from Δw and Δi_{sq} to $\Delta \Phi_r$ are not given, simply because they are practically null. For the identification process, input steps of different amplitude (from 1% to 20%) have been adopted. However, no significant differences have been obtained in the modeling, and consequently no significant difference can be appreciated in the control performance. Thus, in this paper only the models identified with small amplitude step variations are shown in Table 2. In particular, C_x are system models with respect to P_x, where x takes values of 1, 2, 3 and 4. In particular, in this paper, C_1 to C_3 models are used to investigate sensitivity with respect to the rotation speed, while C_1 and C_4 are used to investigate the sensitivity with respect to the load change. As mentioned before, many more models have been used during this research activity.

The set of all the identified models (C_x) is presented in Table 2 using the following transfer function format:

$$G_{input-output} = \mu \frac{(1+\eta s)}{(1+\tau_1 s)(1+\tau_2 s)} \qquad (13)$$

Table 2
Transfer functions of all models

C_x	$G_{\Delta isd\text{-}\Delta\Phi}$	$G_{\Delta isd\text{-}\Delta vdc}$	$G_{\Delta isq\text{-}\Delta vdc}$	$G_{\Delta u\text{-}\Delta vdc}$
C_1	μ=0.1047 η=0 τ_1=0.0847 τ_2=0	μ=84.708 η=0.002 τ_1=0.069 τ_2=0.087	μ=-18.358 η=0 τ_1=0.0695 τ_2=0	μ=1.886 η=0 τ_1=0.069 τ_2=0
C_2	μ=0.1048 η=0 τ_1=0.851 τ_2=0	μ=106.44 η=0.00094 τ_1=0.06878 τ_2=0.0866	μ=-18.503 η=0 τ_1=0.0699 τ_2=0	μ=1.564 η=0 τ_1=0.069 τ_2=0
C_3	μ=0.1045 η=0 τ_1=0.0844 τ_2=0	μ=57.64 η=0.0034 τ_1=0.05718 τ_2=0.09907	μ=-18.448 η=0 τ_1=0.0692 τ_2=0	μ=2.400 η=0 τ_1=0.069 τ_2=0
C_4	μ=0.1058 η=0 τ_1=0.08718 τ_2=0	μ=92.936 η=0.0036 τ_1=0.0761 τ_2=0.1407	μ=-49.155 η=0 τ_1=0.1351 τ_2=0	μ=1.391 η=0 τ_1=0.140 τ_2=0

5. Simulation Results and Discussion

Relevant parameters of the induction generator used in the proposed system are presented in the Appendix. As for simulation and control parameters, the values listed in Table 3 are adopted in all the experiments.

Table 3
Simulation and control parameters

Parameters	Unit	Value
V_{dc}*	V	465
Φ_r*	Wb	0.7
$i_{sd,max}$	A	11
$i_{sq,max}$	A	0
$i_{sd,min}$	A	0
$i_{sq,min}$	A	-28
$\overline{\Delta\imath_{sd,max}}$	A	3
$\overline{\Delta\imath_{sq,max}}$	A	3
$\underline{\Delta\imath_{sd,min}}$	A	-3
$\underline{\Delta\imath_{sq,min}}$	A	-3
T_1	μs	10
T_2	ms	3
H_p	-	40
H_c	-	10
w^V	-	5
w^F	-	1

where $i_{sd,max}$, $i_{sd,min}$, $i_{sq,max}$, $i_{sq,min}$ are maximum, minimum values of i_{sd} and maximum, minimum values of i_{sd} respectively. $\overline{\Delta\imath_{sd,max}}$, $\underline{\Delta\imath_{sd,min}}$, $\overline{\Delta\imath_{sq,max}}$, $\underline{\Delta\imath_{sq,min}}$ are maximum, minimum allowed values of difference between two consecutive control moves of i_{sd}, i_{sq} corresponding. The proposed system and control scheme are simulated using two different sampling times: T_1 is used for the plant including generator model, the PWM rectifier and the hysteresis controller, while the second one T_2 is used for the MPC controller. T_1 is a few microseconds, while one T_2 is a few milliseconds. In our approach, the weights of cost function terms, $w^{R,isd}$, $w^{R,isq}$ are selected much smaller with respect to w^V and w^F in order to drive the controller to focus mainly on the outputs performances.

The experiments performed are shown in the following sections. Basically, they focus on improving performance against load variation and against the rotation speed variation in the system. Different control strategies have been designed and

applied to this purpose. A special attention is given to account for parameter uncertainties and high non-linearity of the generator model used.

5.1. Impact of load changes

The present section shows the results when the load changes in step manner as described in Table 4. Three experiments are performed. The first one is done using an MPC based on a single model, for any value of the outputs. The experiments have been carried out both applying both large and limited variation of the load, in order to investigate the effectiveness of using single-model MPC and the possible need to improve it. The second experiment is performed using a switched MPC approach, where there is a switching between two models to account for large variations of operating conditions. The third experiment is performed through an adaptive MPC controller, in the model parameters have been linearly interpolated and changed following the system. The voltage V_{dc}*, the rotor flux references (Φ_r*) and the rotation speed (Ω) are considered constants (V_{dc}* =465V, Φ_r*= 0.7 Wb and Ω=750 rpm).

Table 4
Large changes of load

t (s)	0-1.5	1.5-3	3-4
R(Ω)	70	140	70

Table 5
Small changes of load

t(s)	T1	T2	T3	T4	T5	T6
R(Ω)	90	110	140	110	90	70

where T1, T2, T3, T4, T5 and T6 are the time instants when the load changes at: 1.5, 2.5, 3.5, 4.5, 5.5 and 6.5 respectively.

5.1.1.Single-model MPC

The blue line in Fig. 5 (the pink line will be discussed in the switched MPC section) represents the controlled DC voltage in case of large load variation (see Table 4), using single-model MPC (C_1). In the initial transient, the DC voltage reaches the reference value in a fast manner (0.47s), then presents an overshoot of about 25.8V at 1.5s and an undershoot of about 21.4V at 3s due to the load changes by +70Ω and -70Ω respectively. Apart from that, the DC voltage is well controlled and it tracks the setpoint for each variation. The settling time is 0.22s approximately. The zoom in this figure shows the first time instant where the DC voltage equal to value of the battery (E=12V) used for the startup of the system. It can also be seen how then the voltage increases once the diode decouples the rectifier from the battery, as soon as the voltage generated at the output of the rectifier is higher than the battery (the same starting way for all the other V_{dc} figures not shown in zoom).

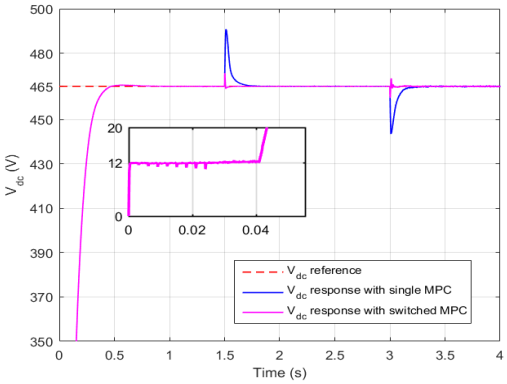

Fig.6. DC Voltage in case of load changes with load large steps using single-model MPC and switched MPC

The controlled rotor flux is presented with a blue line in Fig.7 (it almost completely overlaps with a pink line which will be discussed in the switched MPC section). As it can be seen, the flux is well controlled and following perfectly the setpoint after having reached it in fast manner (0.12s approximately). A very small undershoot is perceived at 1.5s and 3s due to the variation in the load value by -70Ω and +70Ω respectively, as is shown in the zoom.

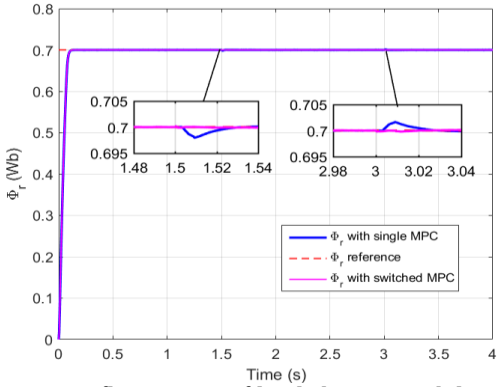

Fig.7. Rotor flux in case of load changes with large steps using both single-model MPC and switched MPC.

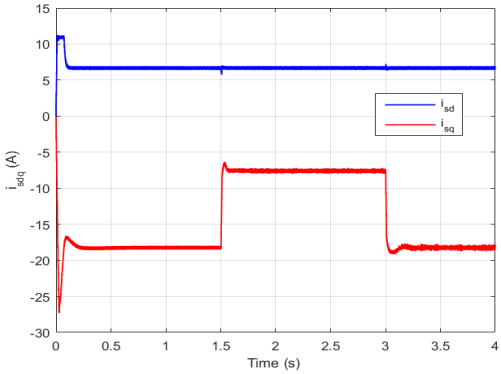

Fig.8. Stator currents i_{sdq} in case of load changes using single-model MPC

Stator currents along d and q axes are presented in Fig. 8. The i_{sd} current shows a similar behavior of the rotor flux. It is almost constant because of the constant speed value, with a very small under/overshoot due the variation of the load at 1.5s and 3s and a peak which reaches the $i_{sd,max}$ value. Since the load is varying, the load variation affects then the value of the requested power, directly related to the VDC, and therefore the active component of the stator current (i_{sq}).

In Fig. 9, the controlled DC voltage due to small changes of the load (see Table 5) is given, using again one single model (C1). In this case, the DC voltage is well controlled and shows small overshoots of about 5.16 V in the average due to the small increasing of the load at 1.5s, 2.5s and 3.5s by 20Ω, 20Ωand 30Ω respectively. It also shows an undershoot of about 4.66 V in the average due to the decreasing in the load at 4.5s 5.5s and 6.5s by 30Ω, 20Ω and 20Ω respectively as shown in Table 5.

The main conclusion that can be drawn is that an MPC architecture is well adequate to control the SEIG even when the load changes, only if the load variations are limited. On the contrary, when the load changes are large, performances decrease significantly.

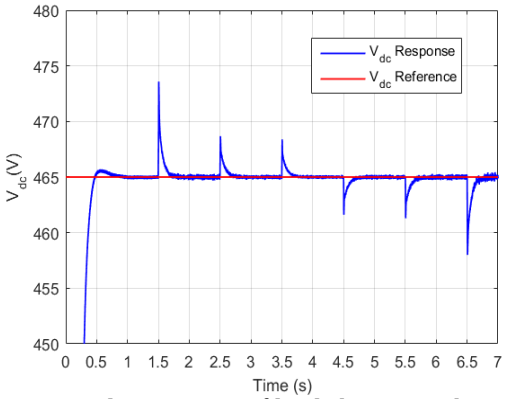

Fig.9. DC Voltage in case of load changes with small step variations using single-model MPC.

5.1.2.Switched MPC

Due to the results of the previous experiments, a switched MPC strategy has been identified in case of large changes of the load. Specially, in order to apply the load large variation of Table 4, and two MPC models have been computed, namely C_1 and C_4. So, accordingly, two switching operations have been performed in the experiment: from C_1 to C_4 and then from C_4 to C_1.

The result of this experiment is given in Fig. 6 where the pink line represents the controlled DC voltage based on the switched MPC. As it can be seen, the DC voltage is controlled much better in comparison with the single-model MPC (blue line). In particular, we have only a small undershoot and overshoot of about 5.5 V (against more than 20) in average due to the large load changes at 1.5(s) and 3(s). In addition the settling time is dramatically improved and faster (0.02s approximately).

The controlled rotor flux is presented in Fig. 7 (pink line) where basically there is no overshoot/undershoot as it can be seen in the zoom frame.

5.1.3.Adaptive MPC

The switched MPC has shown very good performances with respect to the large changes of load. However, if the load takes different values with respect to the operation points around which the models are constructed, the MPC controller will be set-up with anyway a wrong model. For this reason, an adaptive MPC strategy has been designed, with following practical advantages in comparison with the switched MPC:

- The control model related to a bunch of operating points is first computed offline; clearly, the number of operating points will depend on the estimated load range.
- The MPC architecture is parametrized with respect to the plant model.
- The plant model will be interpolated continuously so that the online MPC control is constantly updated with respect to plant.

In particular, as shown in Table 2, each plant model (C_x) presents a set of different transfer functions from inputs to outputs. Taking advantage of the same form of those transfer functions, for each type of transfer function (*i.e.*, $G_{\Delta isd\text{-}\Delta\Phi}$, $G_{\Delta isq\text{-}\Delta\Phi}$, $G_{\Delta isd\text{-}\Delta vdc}$ or $G_{\Delta isq\text{-}\Delta vdc}$), a linear interpolation of gain and time constants is computed as a function of the load. Hence, for any value of load, which is supposed to be estimated by a load sensor, corresponding values of gain and time constants are derived (in other words, the plant model is constructed online for any new operation point). As an example, the gains of $G_{\Delta isq\text{-}\Delta vdc}$ in plant model C_1 and C_4 are used to estimate the gain of the same type transfer function of system model with respect to any load value. Specifically, a linear function that passes through (70Ω, -18.358) and (140Ω, -49.155) is derived as follows:

$$y = -\frac{30.797}{70}x + 12.439 \qquad (14)$$

To test the concrete performance of such a new adaptive MPC architecture, the experiment described in Table 5 has been performed.

Fig. 10 shows that there are high percentage of further reduction of the undershoots and overshoots during the load changes transient with the adaptive MPC strategy with respect to the single-model MPC. In the adaptive MPC case, overshoots and undershoots are less than about 3V in any changes of load.

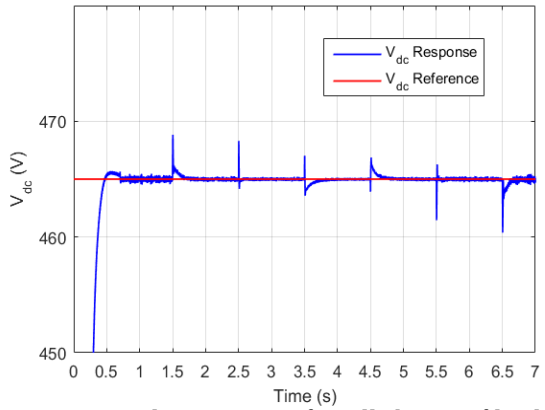

Fig.10. DC Voltage in case of small change of load with adaptive MPC.

Additionally, further simulations on a wider range of the load (from 70Ω to 200Ω) have been considered, and a random load profile containing both small changes and large changes has been applied for 20s. The obtained results show a good maximum overshoot/undershoot of 7V.

5.2. Impact of rotation speed changes

In this section, we present a similar analysis as before, but devoted now to study the impact of rotation speed changes on the controlled DC voltage as well as on the rotor flux. In particular, the driving rotation speed of the induction generator is varied with both large and small variations: with steps of 20% above and below the synchronous speed (Ω = 750 rpm = 78.5398 rad/s) as shown in Table 6 (large variations) and with steps of 10% as shown in Table 7 (small variations). The reference DC voltage and load are kept constants in these experiments (V^*_{dc}=465V, R=70Ω), while the rotor flux reference is changed inversely proportional to the variable speed, which allows the operation of the generator at lower level of saturation in the case of high speeds, as shown in the following equation:

$$\phi_r^* = \frac{\omega_{rat}}{\omega}\phi_{r-rat} \qquad (15)$$

where $\Phi_{r\text{-}rat}$ and $\omega_{rat}$are the rated rotor flux and the synchronous speed, respectively**.**

Table 6
Large changes in rotation speed

t (s)	0-2	2-4	4-6
Ω (rpm)	750	900	600

Table 7
Small changes of rotation speed

t(s)	0-1	1-2	2-3	3-4	4-5
Ω(rpm)	750	825	750	675	750

5.2.1.Single-model MPC

In this experiment, the impact of the rotation speed changes on the DC voltage is investigated using the single-model MPC which based on one linearized model (C1).

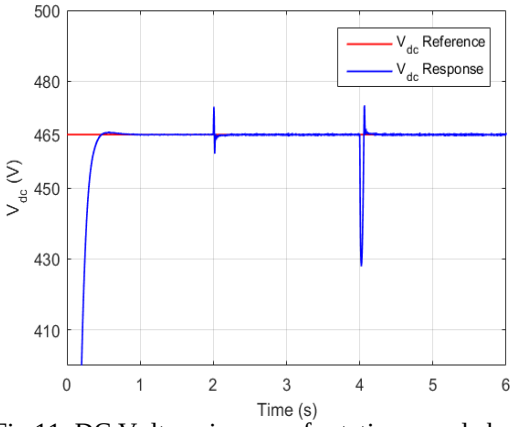

Fig.11. DC Voltage in case of rotation speed changes using single-model MPC.

Fig. 11 represents the controlled DC voltage with a single-model MPC in case of large rotation speed variation. At 4s a big undershoot of about 36.9V is present: this is due to the suddenly decrease of rotation speed of about 34% (from 900 rpm to 600 rpm as shown in the Table 6).

Fig. 12 shows the controlled rotor flux for both cases using single-model and switched MPC presented with blue and pink lines respectively (the pink line will be discussed in Switched MPC section), it is varying inversely proportional to the rotation speed as explained above and expressed in equation (15). The rotor flux is well controlled and follows the rotor flux reference in a good way, with a small under/overshoot in case of using single-model MPC as shown in blue line at 2s and 4s.

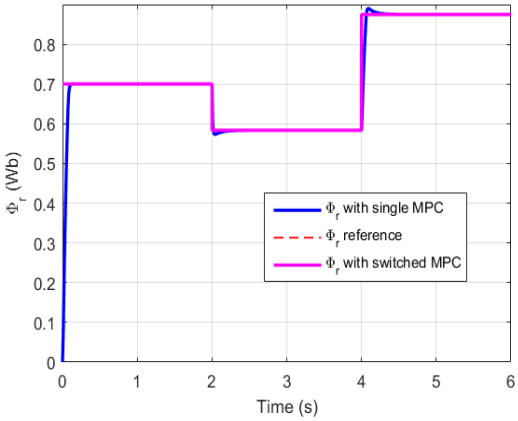

Fig.12. Rotor flux in case of rotation speed changes using single-model MPC and switched MPC

The stator currents I_{sd} and I_{sq} are presented in Fig.13. The reference of the flux is variable according to the speed, so the current i_{sd} adapts to meet the new reference flow for each speed value.

On the contrary, the current i_{sq} shows a weak influence in the variation of the speed which is due to the power of the load which is constant in this case.

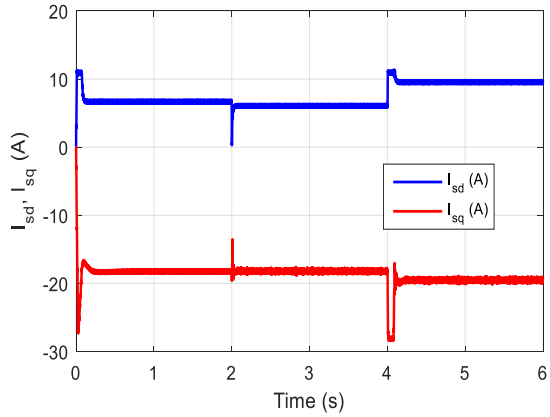

Fig.13. Stator currents I_{sd} I_{sq} in case of rotation speed changes using single-model MPC

As opposed to previous experiments, Fig. 14 presents the controlled DC voltage in case of small rotation speed changes (see Table 7), to check the effectiveness of single-model MPC in case of small variations. The DC voltage is then well controlled and represents small overshoots/undershoot of about 5.5(V) in the average due to the small increasing and decreasing of the rotation speed by 10%.

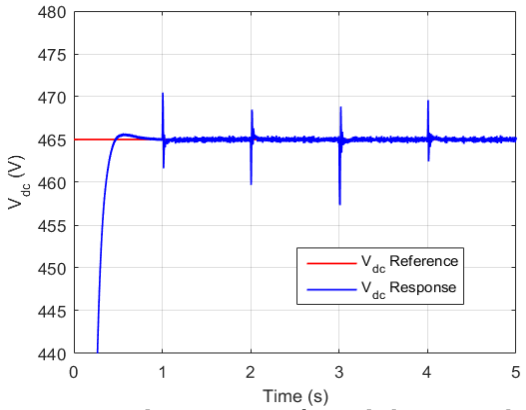

Fig.14. DC Voltage in case of speed changes with small step variations using single-model MPC.

5.2.2.Switched MPC

In this section, a switched MPC strategy is investigated. It is based on the models C_1, C_2 and C_3 computed for the three operational points P_1, P_2 and P_3 of Table 1 which in turn correspond to the three levels of rotation speed shown in Table 6. The controlled DC voltage is given in Fig. 15. An undershoot of about 34.3V is present due to the large rotation speed variation at time 4s (from 900rpm to 600rpm as shown in Table 6VI). Thus, we have an improvement, but of small magnitude, with respect to the single-model MPC.

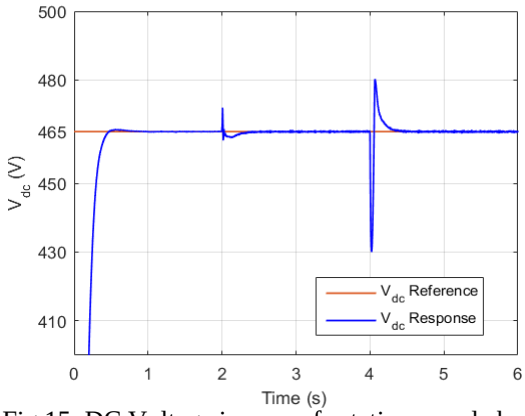

Fig.15. DC Voltage in case of rotation speed changes using switched MPC

Regarding the controlled rotor flux, is presented in Fig 12 with a pink line as mentioned in the previous section, it is perfectly controlled and completely overlapped on the reference rotor flux presented with red dashed line.

5.2.3.Adaptive MPC

Similar to the load case, an adaptive MPC strategy has been designed to test the performance of the system in the scenarios in Table 7. In this case, a quadratic interpolation, instead of a linear interpolation, is exploited to compute gain and time constants, to better follow the nonlinear system dynamics.

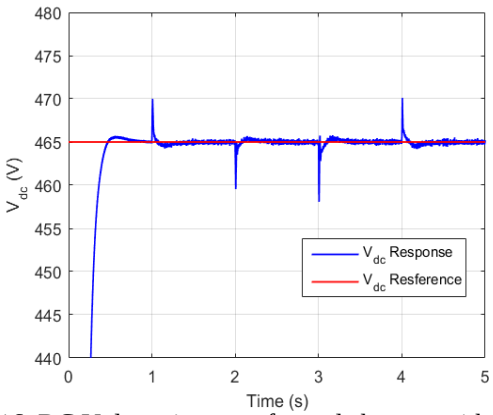

Fig.16. DC Voltage in case of speed changes with small step variations using Adaptive MPC.

The simulation results in Fig.16 show further improvements, but of small entity, between the adaptive MPC strategy and the single-model MPC. Hence, adaptive MPC can be justified only in front of large variations of the rotation speed. However, much better performance have been obtained with pre-filtering actions of the rotation speed (which basically means that there is a non-trivial interaction between the mechanical part control and the electrical part control inside the turbine) and with suitable choices of control parameters (sampling time

and horizons), which prove that there is room for improvement. However, how this can be systematically obtained in a robust way will be analyzed in future work.

6. Conclusion

The paper proposes an interesting application of the Model Predictive Control (MPC) technique to a rotor flux-oriented control for a Self-Exited Induction Generator, attached to a variable speed wind turbine, to be used in a stand-alone system.

The problem addressed in the present paper is tough due to the presence of an excitation system of the autonomous squirrel cage induction generator made of a PWM inverter/rectifier and a single capacitor, and to the saturation effect of the magnetic circuit of the induction generator modeled as an inductance variable with the magnetic current. So, the system model is hybrid and nonlinear.

A wide and thorough investigation shows first an advantage of a linear MPC applied to the nonlinear system model with respect to more traditional controllers (PI). A special focus on large parameters changes shows a further significant improvement in making MPC adapt to load and rotation speed changes, following a switched or even fully adaptive approach. To have an idea of the computational burden, the MPC algorithm can run faster than real-time in Matlab/Simulink on a normal desktop PC, and the adaptation rule is a simple linear/quadratic algebraic operation.

The extremely powerful results of the present research work pave the way to further investigations. A first line focuses on the improvement with respect to the rotation speed, including better tuning of the controller and also a deep analysis of the interaction between the mechanical part control and the electrical part control. Then, the mutual influence of adaptation to load and to rotation speed changes will be investigated, especially in presence of wider range of model uncertainties, as this is often the case in most practical applications. In addition, extension of the application to other IG sizes and models will be performed. Finally, the computational burden will be more clearly analyzed, and sub-optimal solutions will be selected where necessary.

Appendix

Table 8

Parameters of the induction generator

Parameter	Value
P_n	5,5kW
R_s	1.07131Ω
R_r	1.29511Ω
L_s	8.9382mH
L_r	4.8613mH
M	0.10474H
P	4

Acknowledgment

Work partially funded by the European Commission under the Erasmus Mundus Green IT project (Green IT for the benefit of civil society. 3772227-1-2012-ES-ERA MUNDUS-EMA21; Grant Agreement nº 2012-2625/001-001-EMA2).

References

1. Global Wind Energy Council (GWEC).: *Global Wind Report 2016 – Annual market update*.

2. Chauhan Y. K., Jain S. K. and Singh, B.: *Operating performance of static series compensated three-phase self-excited induction generator*. In: International Journal of Electrical Power & Energy Systems, vol. 49 (2013) February 2013, p. 137–148, Canada.

3. Idjdarene, K., Rekioua, D., Rekioua, T., Tounzi, A.: *Performance of an isolated induction generator under unbalanced loads*. In: IEEE Transaction Energy conversion, vol. 25 (2010), No. 2, June 2010, p. 303–311, United States.

4. Seyoum, D., Grantham, C.: *Terminal voltage control of a wind turbine driven isolated induction generator using stator field oriented control.* In: Proceeding of Applied Power Electronics Conference and Exposition APEC '03, September 9-13 2003, Miami Beach, FL, USA, vol. 2, p. 846–852.

5. E. Levi and Y.W. Liao.: *Rotor flux oriented induction machine as a DC power generation*. In: Proceeding of 8th European Conference on Power Electronics and Applications APE'99, 1999, Lausanne, Switzerland, p. 1–8.

6. Idjdarene, K., Rekioua, D., Rekioua, T., Tounzi, A.: *Vector control of autonomous induction generator taking saturation effect into account*. In: Energy Conversion and Management, vol. 49 (2008), July 2008, p. 2609–2617. United Kingdom.

7. Margato, E., Faria, J., Resende, M. J., Palma, J.: *A new control strategy with saturation effect compensation for an autonomous induction generator driven by wind Speed Range Turbines.*In: Energy Conversion and Management, vol. 52(2011), May 2011, p. 2142–2152. United Kingdom.

8. Liao, Y. W., Levi, E.: *Modelling and simulation of a stand-alone induction generator with rotor flux oriented control,* In: Electric Power Systems Research, vol.46(1998), June 1998, p. 141–153, Netherlands.

9. Leidhold, R., Garcia, G., Valla, M. I.*: Field-Oriented Controlled Induction Generator with Loss Minimization.*In: IEEE transactions on industrial electronics, vol. 49(2002), February 2002, p. 147–156, United States.

10. Idjdarene, K., Rekioua, D., Rekioua, T., Tounzi, A.: *Control strategies for an autonomous induction generator taking the saturation effect into account*. In: The 12th European Conference on Power Electronics and Applications EPE'07, September 02-05, 2007, p. 1-10. Aalborg, Denmark,

11. Wang, Y., Wang, Z., Yang J., Pei, R.: *Speed regulation of induction motor using sliding mode control scheme*, In: Industry Applications Conference, vol.

1(2005), October 02-06, 2005, p. 72–76, Kowloon, Hong Kong.
12. Basic, M., Vukadinovic, D., Polic, M.: *Fuzzy DC-voltage controller for a vector controlled stand-alone induction generator,* in: International Journal of Circuit and Signal Processing, 7, 3, (2013) p. 181–190, United kingdom.
13. Krichen, L., Francois, B., Ouali, A.: *A fuzzy logic supervisor for active and reactive power control of a fixed speed wind energy conversion system,* In: Electric Power Systems Research, vol. 78(2008), March 2008, p. 418–424, Netherlands.
14. Meddouri, S., Idjdarene, K., Aberbour, A.:*Fuzzy vector control of isolated generator taking the saturation effect into account*, In: proceeding of International Conference on Electrical Sciences and Technologies in Maghreb CISTEM'14. November 3-6, 2014-Tunis, p. 418–424, Tunisia.
15. Louze, L., Nemmour, A. L., Khezzar, A., Hacil, M. E., Boucherma, M.: *Cascade sliding mode controller for self-excited induction generator*. In: Revue des Energies Renouvelables 12.4 (2009): p.617-626.
16. Aberbour, A., Idjdarene, K., & Tounzi, A.: *sliding mode direct torque and rotor flux control of an isolated induction generator including magnetic saturation*, in: revue roumaine des sciences techniques-serie electrotechnique et energetique, 61(2), p. 142–146, Romania.
17. Soliman, M., Malik, O. P., Westwick,D. T.: *multiple model predictive control for wind turbines with doubly fed induction generators*,In: IEEE Transaction Sustainable energy, vol. 2(2011) July 2011, p. 2375-2380, United States.
18. Kassem, A. M., Yousef, A M.: *Voltage and frequency control of an autonomous hybrid generation system based on linear model predictive control*,In: Sustainable Energy Technologies and Assessments, vol. 4(2013), December 2013 p. 52–61, united kingdom.
19. Kassem, A. M.: *Predictive voltage control of stand alone wind energy conversion system*, In: WSEAS Transaction. Systems and Control, Vol. 7(2012) July 2012, p.97–107, Greece.
20. Li, L-B., Sun, H-X., Chu, J-D., Wang, G-L.: *The predictive control of PMSM based on state space*, In: Proceedings of the IEEE International Conference on Machine Learning and Cybernetics ICMLC'03, vol. 2(2003), November, 2003, p. 859-862, China.
21. Correa, P., Pacas, M., Rodríguez, J.: *A predictive torque control for inverter-fed induction machines*, In: IEEE Transaction Industrial Electronics, vol. 54(2007), no. 2, Apr. 2007, p. 1073–1079, United states.
22. Miranda, H., Cortés, P., Yuz, J. I., Rodríguez, J.: *Predictive torque control of induction machines based on state-space models*, In: IEEE Transaction Industrial Electronics, vol. 56(2009), no. 6, Jun. 2009, p. 1916–1924, United States.
23. Rodríguez, J., Kennel, R. M., Espinoza, J. R., Trincado, M., Silva C. A., Rojas, C. A.: *High-Performance Control Strategies for Electrical Drives: An Experimental Assessment*, In: IEEE Transaction Industrial Electronics, vol. 59(2012), no. 2, February 2012, 812–820, United states.
24. Rekioua, D., Rekioua, T., Idjdarene, K., Tounzi, A.: *An approach for the modeling of an autonomous induction generator taking into account the saturation effect*, In: International Journal of Emerging Electric Power Systems, Vol. 4(2005), Issue 1, june 2005, p. 1-25, United states.
25. Meddouri, S., Dao L. A., Ferrarini, L.: *A predictive control scheme for an autonomous induction generator with saturation effect*, In: Proceedings of International Conference on Clean Electrical Power ICCEP'15, June 16-18, 2015, Taormina, Italy, p. 1118 – 1124.
26. Meddouri, S., Dao L. A., Ferrarini, L.: *Performance analysis of an autonomous induction generator under different operating conditions using predictive control*, In: Proceedings of IEEE International Conference on Automation Science and Engineering CASE'15, August 24-28, 2015, Gothenburg Sweden, p. 1118–1124,
27. Wayne Bequette, B.: *Process control modelling, design and simulation*. In: Prentice Hall PTR (2002), December 26, 2002, p.1- 769, United States.